Bulletin of Mathematical Biology (2022) 84:58
https://doi.org/10.1007/s11538-022-01015-5

Society for Mathematical Biology

ORIGINAL ARTICLE

Mathematical Modeling of Tumor and Cancer Stem Cells Treated with CAR-T Therapy and Inhibition of TGF-β

Ellen R. Swanson[1] · **Emek Köse**[2] · **Elizabeth A. Zollinger**[3] · **Samantha L. Elliott**[4]

Received: 21 July 2021 / Accepted: 22 March 2022 / Published online: 16 April 2022
© The Author(s), under exclusive licence to Society for Mathematical Biology 2022

Abstract

The stem cell hypothesis suggests that there is a small group of malignant cells, the cancer stem cells, that initiate the development of tumors, encourage its growth, and may even be the cause of metastases. Traditional treatments, such as chemotherapy and radiation, primarily target the tumor cells leaving the stem cells to potentially cause a recurrence. Chimeric antigen receptor (CAR) T-cell therapy is a form of immunotherapy where the immune cells are genetically modified to fight the tumor cells. Traditionally, the CAR T-cell therapy has been used to treat blood cancers and only recently has shown promising results against solid tumors. We create an ordinary differential equations model which allows for the infusion of trained CAR-T cells to specifically attack the cancer stem cells that are present in the solid tumor microenvironment. Additionally, we incorporate the influence of TGF-β which inhibits the CAR-T cells and thus promotes the growth of the tumor. We verify the model by comparing it to available data and then examine combinations of CAR-T cell treatment targeting both non-stem and stem cancer cells and a treatment that reduces the effectiveness of TGF-β to determine the scenarios that eliminate the tumor.

Keywords Mathematical oncology · Cancer stem cell · CAR-T immunotherapy · Transforming growth protein

✉ Ellen R. Swanson
ellen.swanson@centre.edu

1 Department of Mathematics, Centre College, Danville, KY, USA

2 Department of Mathematics and Computer Science, St. Mary's College of Maryland, St. Mary's City, MD, USA

3 Department of Mathematics and Computer Science, St. Joseph's College, Brooklyn, NY, USA

4 Department of Biology, St. Mary's College of Maryland, St. Mary's City, MD, USA

1 Introduction

An estimated 39.5% of people in the USA will be diagnosed with cancer during their lifetime, with over 1.8 million new cases diagnosed each year. The annual financial burden in the USA is $150.8 billion (2018), and costs continue to rise due to cutting-edge technologies that provide personalized patient treatments (National Cancer Institute 2020). These recent advances provide multiple fronts by which to combat cancer growth, with particular focus on interactions between cancer cells, the immune system and the tissue microenvironment (reviewed in Lee et al. (2018); Morganti et al. (2019); Wang et al. (2018)). With advances in biomarker research, targeted therapies increase treatment efficacy and reduce patient side effects (Bashraheel et al. 2020). This has resulted in very specific treatments for individual patients based upon the cancer's genetic profile.

Cancer cells themselves consist of a heterogeneous population of differentiated or partially differentiated cells which often undergo rapid proliferation and mutation. Selective pressure due to cancer therapeutics (e.g., chemotherapy) can cause drug resistance by cancer cells; thus, combination therapies are often used to minimize this risk (Bashraheel et al. 2020). The discovery of cancer stem cells (CSCs), undifferentiated cells which often avoid traditional cancer therapeutics due to their lower proliferation rate, adds yet another cellular sub-population that must be addressed to effectively eliminate the cancer burden of the patient (reviewed in (Clara et al. 2020)).

More recent therapeutic approaches focus upon contributions of the immune system and the tissue microenvironment (TME), which can promote or prevent cancer cell growth. The advent of chimeric antigen T-cells (CAR-T cells), which are genetically engineered from the patient's own immune cells, has revolutionized cancer medicine. However, while successful against various leukemias and lymphomas, CAR-T cell therapy of solid tumors has lagged behind due to issues of penetrance and inhibition (reviewed in Scarfò and Maus (2017)). This is predominantly caused by the immunosuppressive TME, both from tumor immune evasion (e.g., TGF-β and IL-10 expression) and direct immune system regulation (e.g., regulatory T cells (Tregs), immune checkpoint inhibitors like PD-L1) (reviewed in (Mortezaee 2020)).

While mathematical modeling is a robust method to predict outcomes of cancer therapeutics, there are few models that address the complex contributions of the immune system, combination therapeutics, and the tumor microenvironment together. Rather, most studies examine individual pieces of the complex biological system. The complexities of the cancer stem cell evolution, division and differentiation are modeled in Piotrowska et al. (2008); Weekes et al. (2014); Johnston et al. (2010); Weiss et al. (2017); Beretta et al. (2012). The models given in Hillen et al. (2013) and Fasano et al. (2016) address the tumor paradox, where a high mortality in non-stem cancer cells results in an increased rate of tumor growth, also known as the stem cell hypothesis.

Immunotherapies utilize the body's own immune system to generate a response to the tumor, often using genetic manipulation of the patient's immune components. These include mathematical models of immune checkpoint inhibitors (Radunskaya et al. 2018), dendritic cell vaccines (Köse et al. 2017; Sigal et al. 2019), and CAR-T cells (Sahoo et al. 2020).

Models of combination therapies are quite limited. Sigal et al. explore the efficacy of an immunotherapy which specifically targets either the tumor or cancer stem cells and combine it with chemotherapy (Sigal et al. 2019). They find this combination is essential in order for the tumor and stem cells to be completely eliminated.

Some mathematical models address the immunosuppressive tumor microenvironment (TME), which influences the growth of the tumor (Louzoun et al. 2014). Wilson et al. specifically explore the impacts of TGF-β (Wilson and Levy 2012). Elliott et al. incorporate the influence of TGF-β on both cancer stem cells and tumor cells (Elliott et al. 2019). Additionally, they investigate a chemotherapy treatment attacking the cancer cells.

In this paper, we combine these multiple elements to model a more complex, yet more biologically relevant, system of tumor growth. We focus on TGF-β inhibitors and two specific immunotherapies: CAR T-cell therapy targeting tumor and cancer stem cells individually. We explore combination therapies with the goal of creating a treatment that is gentler on the patients. In Sect. 2, we present the model of ordinary differential equations. We analyze the model in Sect. 3 with a sensitivity analysis and in Sect. 4 with a stability analysis. In Sect. 5 we consider different treatment scenarios and compare to data of tumor growth in mice. Using the results of these studies we suggest a potential treatment that combines immunotherapies targeting tumor and stem cells that inhibits the effects of TGF-β on tumor growth. These forms of therapies are known to cause fewer side effects on the patient. Thus we present an effective, better-tolerated treatment scenario.

2 Model

We consider the growth of the tumor (T) and cancer stem cells (S) when attacked by CAR-T cells, a form of effector cell, designed to either specifically target the tumor (E) or cancer stem cells (C) while being regulated by TGF-β (B) and regulatory T-Cells (R). The interactions are displayed in Fig. 1 and described by

$$\frac{dS}{dt} = \boxed{pv_0}\left(1 - \frac{T+S}{K}\right)S - \mu_{CS}CS \tag{1a}$$

$$\frac{dT}{dt} = \eta T\left(1 - \frac{(T+S)}{K}\right) + (1-p)v_0\left(1 - \frac{T+S}{K}\right)S - \mu_{ET}\frac{TE}{1+c_1B} \tag{1b}$$

$$\frac{dE}{dt} = v_{ET}(t) + bE + \frac{fET}{1+c_3TB} - \mu_{RE}RE - \delta_E E - rE \tag{1c}$$

$$\frac{dC}{dt} = v_{CT}(t) + bC + f\frac{CS}{1+c_3TB} - \mu_{RC}RC - \delta_{CT}C \tag{1d}$$

$$\frac{dB}{dt} = \frac{aT^2}{c_2+T^2} + \alpha_{RB}R - \delta_B B \tag{1e}$$

$$\frac{dR}{dt} = rE - \delta_R R. \tag{1f}$$

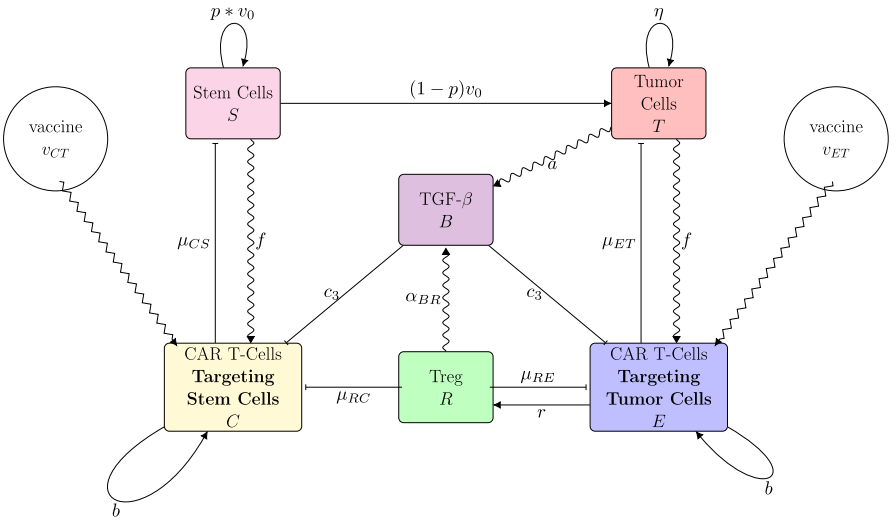

Fig. 1 Model diagram for Eq. (1) (color figure online)

The first equation represents the change in the cancer stem cell population (S) size with respect to time. The first term represents the logistic growth of the cancer stem cells where v_0 is the frequency that stem cells divide and p is the probability that a stem cell is produced from that division. We implement logistic growth hindered by the total number of cancer cells, since both the tumor and stem cells compete for resources within the tumor environment. Other studies implement feedback functions, in the form of Hill functions, on the reproduction parameters rather than logistic growth (Renardy et al. 2018; Rodriguez-Brenes et al. 2017; Wodarz 2018; Liu et al. 2013). However, Hill functions generally do not have a physical explanation (Rodriguez-Brenes et al. 2017; Renardy et al. 2018), whereas growth of the tumor is known to be limited by the resources available which correlates to the number of cells in the tumor environment. As done by Youssefpour et al. (2012), we define p to be the probability that a stem cell division produces stem cells. We ignore the intricate details of symmetric versus asymmetric division, as thoroughly described in Liu et al. (2013), Elliott et al. (2019), Sigal et al. (2019) but rather focus on the overall percentage of stem cells created. The killing of the cancer stem cells (S) by CAR-T cells that target the CSC (C) is incorporated in the second term. One characteristic of stem cells is their longevity which is why a natural death rate is not included.

The growth of the tumor is described in Eq. (1b). The first term describes the logistic growth of the tumor. The differentiation of stem cells into tumor cells is included in the second term. The last term represents the death of the tumor cells by the CAR-T cells, but this death is limited by the presence of TGF-β.

The next two Eqs. (1c, 1d) represent the CAR-T cells, (E) are the CAR-T cells that target the tumor, while (C) are the CAR-T cells that target the stem cells. The first term in each equation allows for treatment to be included. The second term is the basal growth of the respective CAR-T cells. The third term represents the increase in CAR-T cells due to interaction with the corresponding cancer cells. This growth is inhibited

by both the tumor cells and TGF-β, so the term is multiplied by $(1 + c_3 T B)^{-1}$ as in (Wilson and Levy 2012). One job of the regulatory T-cells is to ensure that the immune system does not go into overdrive; this regulatory behavior is accounted for in the fourth terms. The δ terms represent the natural death rate of the CAR-T cells. Effector cells can transition into a regulatory capacity as seen in the final term in the (E) equation.

Transforming growth factor, TGF-β (B), is a cytokine that provides a defense for the tumor cells with a primary role of decreasing the effectiveness of effector cells on killing the tumor cells. It also aids the tumor by reducing the instigation of effector cell growth that occurs when interaction occurs between effector and cancer cells. Tumor cells produce TGF-β to stimulate angiogenesis, particularly when a tumor is large because in this case the tumor cells are suffering from a lack of necessary nutrients, like oxygen. This growth is the first term of the (B) equation which is equivalent to that used by Arciero and Kirschner (2004) and Wilson and Levy (2012). The second term is the support of the TGF-β by regulatory T-cells (R). And the final term is the natural elimination of TGF-β.

The regulatory T-cell compartment is populated by the transition of the CAR-T cells and is naturally depleted as represented in (1f).

3 Sensitivity Analysis

We examine the sensitivity of System (1) by finding the Partially Ranked Correlation Coefficients (PRCC) which measure the impact of a parameter on the system independent of the other parameters (Marino et al. 2008). The parameters that have a substantial impact on at least one variable are shown in Fig. 2. In this sensitivity analysis, we use the parameters from Table 1 for Zhang 2019 because this situation incorporates both types of effector cells and thus is working with the full system (Zhang et al. 2019). We find that p and v_0 have the biggest impact on the cancer stem cells, while the tumor is influenced substantially by η. We focus on these three parameters in Sect. 5 when fitting the model to data since the data are primarily for tumor and cancer stem cells.

Identifiability analysis reveals that with tumor data, we are able to reliably fit three parameters; $v_0,\ \eta,\ f$ or $p, \eta,\ f$. We have used the `FME` package in `R` Soetaert and Petzoldt (2010). The collinearity or the identifiability score of these two sets of parameters is below 20 and thus is identifiable by the provided data.

4 Stability Analysis

System (1) yields four meaningful, real-valued equilibrium points. The corresponding eigenvalues and eigenvectors for each equilibrium point are given in Appendix.

There is a line of co-existing equilibrium with tumor and immune cells, which is

$$(S^*, T^*, E^*, C^*, B^*, R^*) = \left(K - T^*, T^*, 0, 0, \frac{a(T^*)^2}{\left(c_2 + (T^*)^2\right)\delta_B}, 0 \right).$$

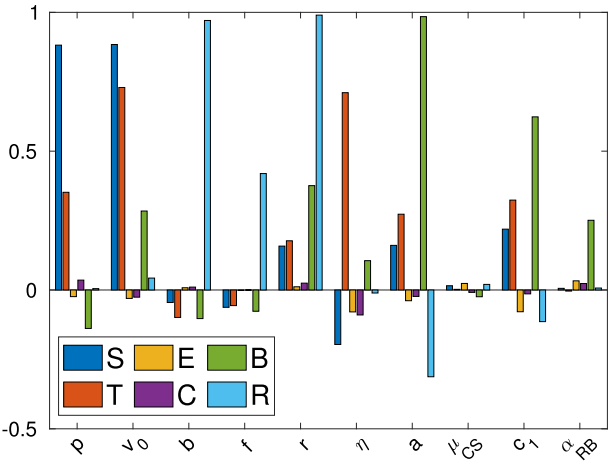

Fig. 2 The Partially Ranked Correlation Coefficients (PRCC) for Eq. (1) using Zhang2019 parameters from Table 1 (color figure online)

This is the equilibrium approached in Fig. 3, using the parameters in Table 1. We assume initially that the number of cancer stem cells is 1% of the number of tumor cells. Both the cancer stem cells and the tumor cells initially increase in number, approximately exponentially before approaching the equilibrium values. The TGF-β increases as expected since the tumor continues to grow and thus creating more TGF-β. With the absence of effector cells, the regulatory T-cells are eventually eliminated though at a slow rate. When there are no effector cells $E^* = C^* = 0$, System (1) reduces dramatically. While the regulatory T-cells are eliminated, the TGF-β levels off to $B^* = \frac{aT^2}{\delta_B(c_2+T^2)} = 845.3$ with the Tang2020 parameters which is the value observed in Fig. 3c and the equilibrium value predicted by the stability analysis (Tang et al. 2020). Additionally, we find equilibrium $T^* = K - S^* = 9.9 \times 10^8$ and $S^* = K - T^* = 1.0 \times 10^7$. Note that $T^* + S^* = K = 10^9$.

There are two positive eigenvalues, both of which point to an inverse relationship between the cancer stem cells and the tumor. One of them also repels in a direction of increasing CAR-T cells, since if injected into the body, they proliferate; meanwhile, the other eigenvector indicates a decreasing effector cell population, as tumor grows. Of the two stable directions, one shows a balance between tumor and cancer stem cells, while the other shows an attraction parallel to TGF-β axis.

5 Treatment

We explore different forms of cancers including metastatic lung cancer (Tang et al. 2020), gastric carcinoma (KATO III) (Han et al. 2021), and colorectal carcinoma (HT29) (Zhang et al. 2019). We compare numerical simulations to data from experiments presented in Tang et al. (2020),Han et al. (2021),Zhang et al. (2019). When available we include error bars corresponding to results of the experiments.

Table 1 The parameter values used in the model for different cancers, represented by different sets of data

Parameter	Units	Data from Tang et al. (2020)	Data from Han et al. (2021)	Data from Zhang et al. (2019)	Literature values
p	1	0.1351	0.4063	0.4063	–
v_0	$\frac{1}{\text{Day}}$	0.3628	0.4218	0.2895	0.5η (Liu et al. 2013)
K	Cells	10^9	10^9	10^9	–
μ_{CS}	$\frac{1}{\text{Cell}\times\text{Day}}$	10^{-6}	10^{-6}	4×10^{-6}	–
η	$\frac{1}{\text{Day}}$	0.0454	0.1661	0.1133	0.1946 (Wilson and Levy 2012)
μ_{ET}	$\frac{1}{\text{Cell}\times\text{Day}}$	2×10^{-5}	10^{-5}	2×10^{-5}	10^{-5} (Wilson and Levy 2012)
c_1	$\frac{\text{mL}}{\text{ng}}$	100	100	100	100 (Wilson and Levy 2012)
b	$\frac{1}{\text{Day}}$	0.4843	0.4254	0.4254	–
f	$\frac{1}{\text{Cell}\times\text{Day}}$	0.0011	0.002	0.002	–
c_3	$\frac{\text{mL}}{\text{ng}\times\text{Cell}}$	0.1224	0.1224	0.1224	–
μ_{RE}	$\frac{1}{\text{Cell}\times\text{Day}}$	10^{-5}	10^{-5}	10^{-5}	10^{-5} (Wilson and Levy 2012)
δ_E	$\frac{1}{\text{Day}}$	10^{-5}	10^{-5}	10^{-5}	10^{-5} (Wilson and Levy 2012)
r	$\frac{1}{\text{Day}}$	0.0125	0.01	0.01	0.01 (Wilson and Levy 2012)
μ_{RC}	$\frac{1}{\text{Cell}\times\text{Day}}$	10^{-5}	10^{-5}	10^{-5}	–
δ_{CT}	$\frac{1}{\text{Day}}$	10^{-4}	10^{-4}	10^{-4}	$< 10^{-3}$(Sahoo et al. 2020)
a	$\frac{ng}{\text{Day}\times\text{mL}}$	0.5917	0.6011	0.6011	–
c_2	$Cell^2$	1.875×10^9	1.875×10^9	1.875×10^9	–
α_{RB}	$\frac{1}{\text{Day}}$	10^{-8}	10^{-7}	10^{-7}	–
δ_B	$\frac{1}{\text{Day}}$	7×10^{-4}	7×10^{-4}	7×10^{-4}	7×10^{-4} Arciero and Kirschner (2004)
δ_R	$\frac{1}{\text{Day}}$	10^{-5}	10^{-5}	10^{-5}	10^{-5}(Wilson and Levy 2012)

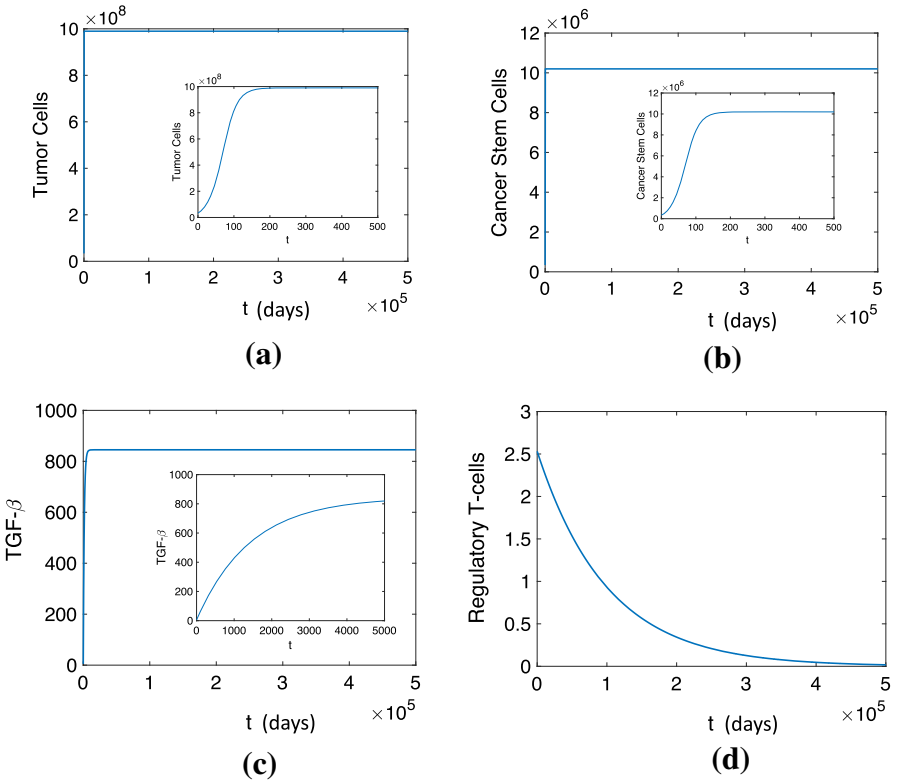

Fig. 3 The long-term behavior of **a** tumor cells, **b** cancer stem cells, **c** TGF-β, and **d** regulatory T-cells using the Tang2020 parameters in Table 1 and initial conditions $T(0) = 3.4 \times 10^7$, $S(0) = .01 * T(0)$, $B(0) = 5$, $R(0) = 2.5$ and $E(0) = C(0) = 0$ (color figure online)

5.1 No Treatment

Using metastatic lung cancer data (Tang et al. 2020), we are able to find fitting parameters. This study provided tumor fold size with an initial tumor that was $200-300$ mm^3, so we assume $T_0 = 250$ mm^3. We convert tumor fold size to number of cells using the following relationship

$$\text{Tumor Data Cell} = \frac{\text{Tumor Fold Size} \times 250\text{mm}^3 \times 10^9\ \mu\text{m}^3}{20^3\ \mu\text{m}^3}. \tag{2}$$

In this conversion we are assuming that the tumor is approximately a cube with equal length sides and that the dimension of one cell is $20\mu m$. When there is no treatment, we assume there are no functioning effector cells, meaning we take $E(0) = 0$. Cancer stem cells make up anywhere from 0.03 to 100% of the tumor (Marotta and Polyak 2009; Tomasetti and Vogelstein 2015), thus necessitating an estimation. We assume that cancer cells in the tumor environment satisfy a ratio of 1:100 (CSC:Tumor) because this ratio represents a value in close approximation to many tissue types in Tomasetti

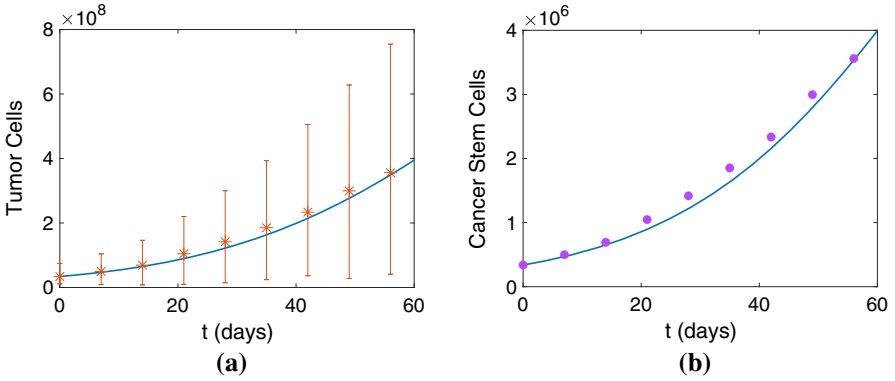

Fig. 4 Comparing results from Tang et al. (2020) of metastatic lung cancer cells to the simulation of (1) in the absence of functioning effector cells, E(0)=0. **a** total number of tumor cells ($T+S$) along with tumor cell data (*) and error bars and **b** stem cells, we assume stem cells are 1% of the tumor cells for the calculated data (•) (color figure online)

and Vogelstein (2015). Additionally, we use the data to set the initial conditions $T(0) = 3.4 \times 10^7$ and $S(0) = .01 * T(0)$. We take $B(0) = 5$ and $R(0) = 2.5$. In order to fit the parameters we use the MATLAB function *fminsearch* and compare the simulation output to the data in which that parameter has the biggest impact, as determined by the PRCC. We primarily use the CSC data to fit the parameters p and v_0. The remainder of the parameters are fit by comparing the simulation of the total number of cancer cells, the sum of tumor and stem cells, to the tumor data. We find that η has the biggest impact on the solution, as predicted by the PRCC. Note that multiple parameters are irrelevant since there are no effector cells. Figure 4 displays the good agreement between the simulation and tumor growth in the absence of functioning effector cells.

5.2 Treatment Targeting the Tumor

Tang et al. considered various treatments using different types of CAR-T cells. Before examining the impact of these CAR-T cells, they looked at the proliferation of the effector cells in a Petri dish (Tang et al. 2020). We use the M28z CAR-T cells to fit the most relevant parameters for the effector cells, specifically b, r, f, α_{RB}. Figure 5 shows the agreement between the simulation of the number of M28z CAR-T cells and the in vitro experiment. The parameters are listed in Table 1, alongside the values fit when there were no effector cells present. Based on data available, we combine results from in vitro and in vivo experiments. In particular, the number of effector cells was only collected through in vitro experiments which provide ideal growing conditions without a suppressive microenvironment. Thus the number of effector cells present in vivo would be an overestimate of the number of effector cells within the mice. Using insight from the in vitro experiments of how the effector cells proliferate, we can better describe the in vivo dynamics of the tumor and immune cells.

In terms of treatment, the M28z CAR-T cells specifically attack the tumor cells. Two doses of 5×10^6 M28z cells are injected through IV into the mouse on Day 0 and

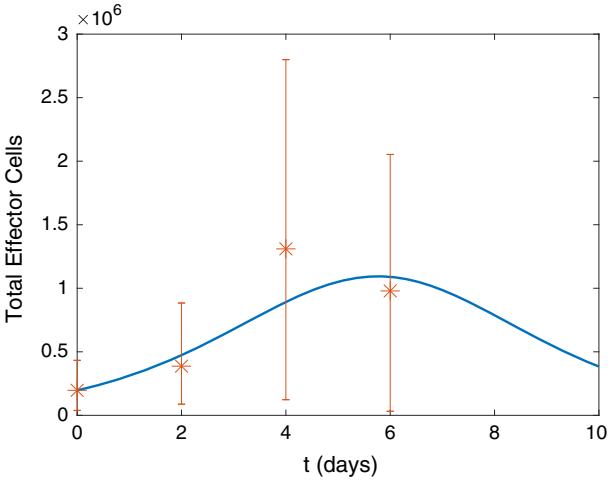

Fig. 5 Number of simulated effector cells using Eq. (1) and number of effector cells in vitro. The initial condition is the number of in vitro effector cells on Day 0, E(0)=19700, while the other variables are set by the in vivo experiment described below, $T(0) = 3.4 \times 10^7$, $S(0) = 0.01 \times T(0)$, $B(0) = 5$, $R(0) = 2.5$, $C(0) = 0$ (color figure online)

Day 7. Equations (1) with the parameters in Table 1 along with the data for number of tumor cells in a mouse are shown in Fig. 6. We see basic agreement between the data and simulation with the simulation initially demonstrating a slightly stronger response to the treatment than the tumors within the mice. Comparing the tumor growth without treatment, Fig 4, and with tumor targeted treatment, Fig 6, we see the growth of the tumor is slowed by the CAR-T treatment.

5.3 Treatment Targeting the Tumor and Inhibiting TGF-β

TGF-β is produced by the tumor cells and ultimately aids in the growth of the tumor by inhibiting the immune system. Specifically, TGF-β inhibits the proliferation of effector cells and also reduces the efficiency of the effector cells in killing the tumor cells. We explore the impacts of TGF-β inhibition on the growth of a tumor. TGF-β is less effective at inhibiting the proliferation of the effector cells due to the presence of the tumor which we account for by reducing the parameter $c_3 = 0.01$. Additionally, we take $c_1 = 10$ to account for weaker inhibition of effector cells attacking tumor cells. For both parameters, we reduced the effectiveness of the TGF-β in inhibiting the effector cells to 10% of uninhibited TGF-β. We also alter the parameters $r = 10^{-4}$, $\mu_{ET} = 10^{-7}$ and $\delta_R = 0.1$. The reduction of r represents that fewer effector cells are becoming regulatory T-cells as evidenced in Moo-Young et al. (2009), Polanczyk et al. (2019). Additionally, we assume that the effector cells are slightly less effective at killing the tumor cells. By reducing the impact of TGF-β on the effector cells in our model, we cause the effector cells to be too effective when in reality there are other proteins that also inhibit the effectors such as CTLA-4. For the other parameters, we use the values in Table 1. Figure 7 shows a comparison between the same treatment described in Sect.

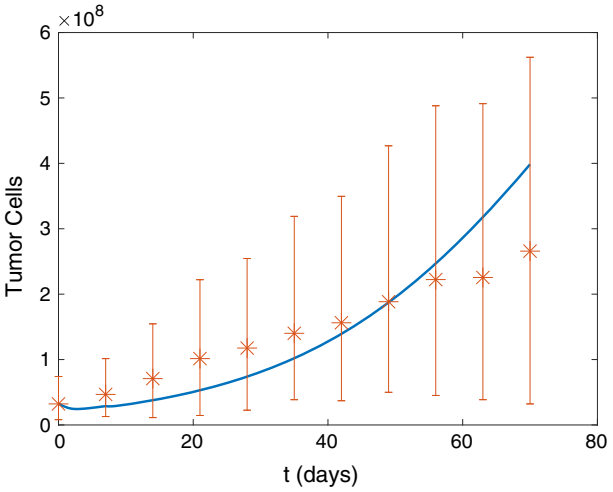

Fig. 6 Number of metastatic lung cancer tumor cells from (Tang et al. 2020) and simulation of total number of tumor cells $(T+S)$ using (1). The initial conditions are $T(0) = 3.4 \times 10^7$, $S(0) = 0.01 \times T(0)$, $B(0) = 5$, $R(0) = 2.5$, $C(0) = 0$. Two treatment doses of 5×10^6 M28z CAR-T cells, corresponding to E, are injected through I.V. on Days 0 and 7 causing $E(0) = 5 \times 10^6$ (color figure online)

5.2 and that treatment with the addition of an inhibition of the TGF-β. The tumor grows slower when the TGF-β is inhibited because the effector cells are more effective at killing the tumor cells. However, the tumor continues to grow in both scenarios. With the reduction of tumor cells, the cancer stem cells proliferate faster because they are trying to repopulate the tumor. The effector cells targeting the tumor level off at a higher value when the TGF-β is inhibited and exhibit oscillatory behavior as they approach a steady-state value. Fewer effector cells transition to regulatory T-cells because they are committed to fight the tumor, but the regulatory T-cells population still follows the oscillatory behavior of the effector cells. The TGF-β population is the same between the two situations because the amount of TGF-β present is not altered; rather, the effectiveness is reduced. This comparison suggests that the inhibition of TGF-β slows the growth of the tumor but still is not successful at completely eliminating the tumor.

We further investigate two additional cancers. Every type of cancer has its own specific growing mechanisms and rates. In the following treatments we consider different types of lung, stomach, and colorectal cancers. For each new type of cancer, we must find the relevant parameters to describe the growth of that cancer. Using the control data, we find the parameters for the growth of each tumor. We work with initial conditions $S(0) = 0.01 * T0, T(0) = InitialTumorData, E(0) = 0, C(0) = 0, B(0) = 5$ and $R(0) = 2.53$. The assumption that there are initially no effector cells is a simplification that acknowledges the ineffective lymphocyte response to the tumor; this is indeed a "worst case scenario" which underestimates overall effect of the immune response on the tumor. Notice that the biggest difference between the parameters values, displayed in Table 1, are for the parameters p and v_0, the probability of creating a stem cell and the frequency of division of the stem cells. Otherwise the parameter

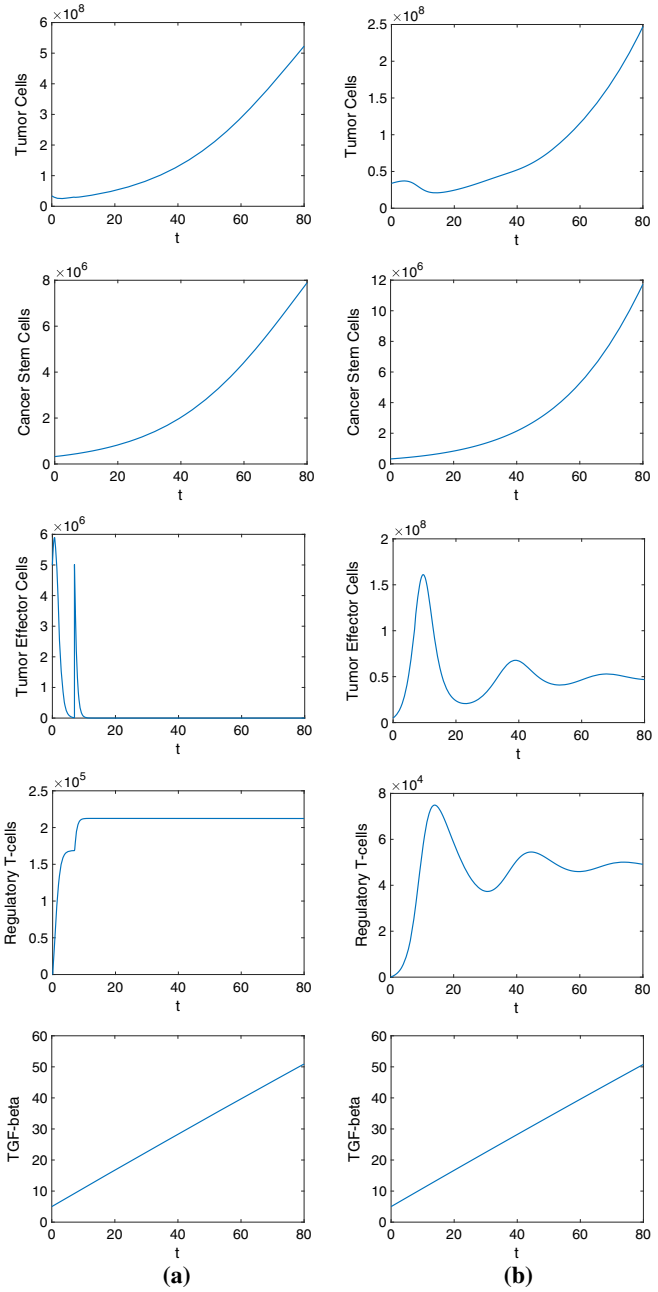

Fig. 7 Comparison of the number of tumor cells, cancer stem cells, T-cells targeting the tumor, regulatory T-cells, and amount of TGF-β when **(a)** treatment targets only the tumor with two treatment doses of 5×10^6 M28z CAR-T cells, corresponding to E are injected through IV on Days 0 and 7. **(b)** treatment targets the tumor and inhibits the TGF-β with two treatment doses of 5×10^6 M28z-KTO CAR-T cells, corresponding to E are injected through IV on Days 0 and 7. The parameters in Table 1 are used, except $c_1 - 10,\ c_3 = 0.01,\ r = 10^{-4},\ \mu_{ET} = 2 \times 10^{-6},$ and $\delta_R = 0.01$ (color figure online)

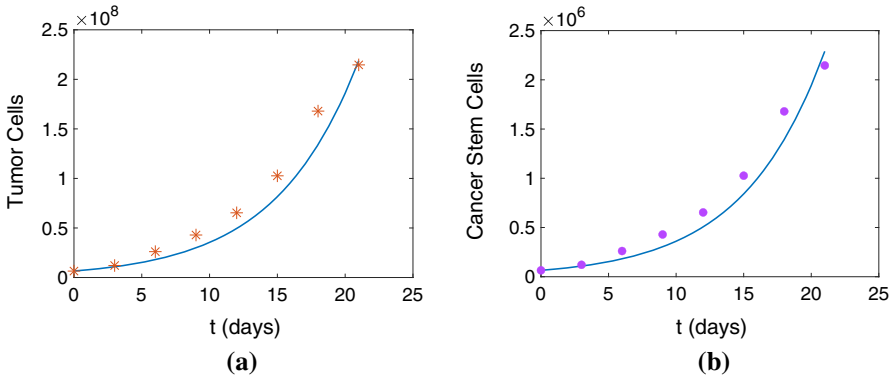

Fig. 8 Number of gastric carcinoma (KATO-III) cells from (Han et al. 2021) and simulations of (1) when no effector cells are present. **(a)** Total number of tumor cells ($T + S$) along with tumor cell data (*). **(b)** Stem cells, we assume stem cells are 1% of the tumor cells for the calculated data (·) (color figure online)

values are similar, suggesting (1) is a robust model. We then initiate the treatment and compare the results to the growth of the tumor in mice undergoing that treatment.

5.4 Treatment Targeting the Cancer Stem Cells

Han et al. (2021) examine a treatment that targets various stomach cancers. One treatment is CD133 CAR T cells which target the cancer stem cells (Liou 2019). Once a tumor reaches approximately 50 mm^3 the treatment study begins, defined as day 0. Figure 8 shows the growth of the tumor and stem cells when no treatment is given. The parameters for the simulation are given in Table 1 and there are no effector cells initially, $E(0) = C(0) = 0$. Figure 9 shows the growth of the tumor and stem cells when a treatment of 2.5×10^6 CD133 CAR T cells is injected into the mice on day 3 and day 12. While the stem cells are quickly eliminated, the tumor is not substantially reduced suggesting that treatment only targeting the stem cells is not effective.

5.5 Treatment Targeting Tumor and Cancer Stem Cells

We next consider treatments that attack both the tumor cells and cancer stem cells for colorectal carcinoma (HT29). The treatment of Ep-CAM-specific CAR-T cells targets both the tumor cells and the cancer stem cells (Eyvazi et al. 2018). We assume there are no effector cells, $E(0) = C(0) = 0$, when fitting the control data and determining the parameter values given in Table 1. The mice were inoculated with approximately $T(0) = 5 \times 10^6$ HT29 tumor cells and $S(0) = 5 \times 10^4$ stem cells on day 0. Figure 10 shows the number of total tumor cells and cancer stem cells in the case where the CAR-T cells are not introduced. Figure 11 shows the number of total tumor cells and cancer stem cells when $E(0) = 2 \times 10^7$ and $C(0) = 2 \times 10^5$ effector cells are presented at the same time as the cancer cells to the mouse. In the experiments reported in Zhang et al. (2019), the ratio between effector cells and tumor cells (E:T) is 4:1. We

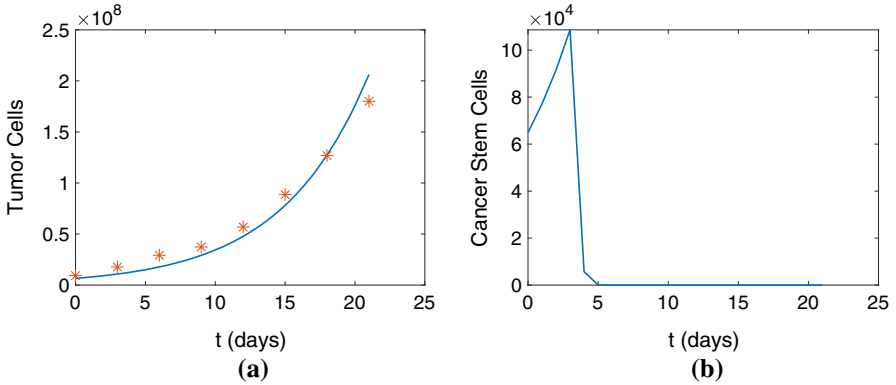

Fig. 9 Number of gastric carcinoma (KATO-III) cells from (Han et al. 2021) and simulations of (1) for a treatment of AXL-specific CAR-T targeting the cancer stem cells with injections of $v_{CT} = 2.5 \times 10^6$ effector cells (C) on days 3 and 12. **(a)** Total number of tumor cells ($T + S$), (*). **(b)** Stem cells (color figure online)

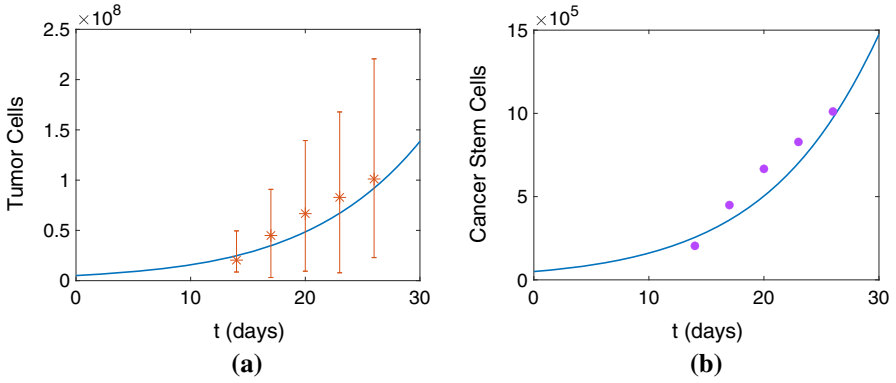

Fig. 10 Number of colorectal carcinoma (HT29) cells from Zhang et al. (2019) and simulations of (1) when no effector cells are present. $E(0) = C(0) = 0$ and $T(0) = 5 \times 10^6$ and $S(0) = 5 \times 10^4$. **(a)** Total number of tumor cells ($T + S$) along with data of tumor cells (*) and corresponding error bars. **(b)** Stem cells, we assume stem cells are 1% of the tumor cells for the calculated data (•) (color figure online)

use this ratio to set the initial conditions for both types of effector cells, E and C. We specifically relate the effector cells that attack the stem cells to the number of cancer stem cells, C:S. Both in the treatment and control cases, the model well captures the growth of the tumor and the number of cancer stem cells.

5.6 Combination Treatment

In all the of the treatments considered, the tumor and stem cells still ultimately grow. Here we consider the additional treatment of effector cells attacking both the tumor and the stem cells combined with reducing the capability of TGF-β to inhibit the effector cells. In all cases, we introduce a treatment on days 0, 7, 14. The treatment for effector cells attacking the tumor is $E = 2 \times 10^7$ and effector cells attacking the

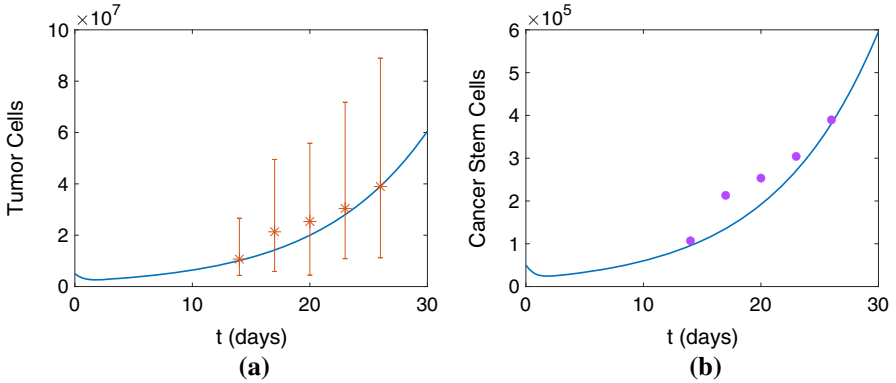

Fig. 11 Number of colorectal carcinoma (HT29) cells from Zhang et al. (2019) and simulations of (1) for a treatment targeting both the cancer stem cells and the tumor cells. On day 0, effector cells were injected, $E(0) = 2 \times 10^7$ and $C(0) = 2 \times 10^5$. **(a)** Total number of tumor cells $(T + S)$ along with data of tumor cells (*) and corresponding error bars. **(b)** Stem cells, we assume stem cells are 1% of the tumor cells for the calculated data (•) (color figure online)

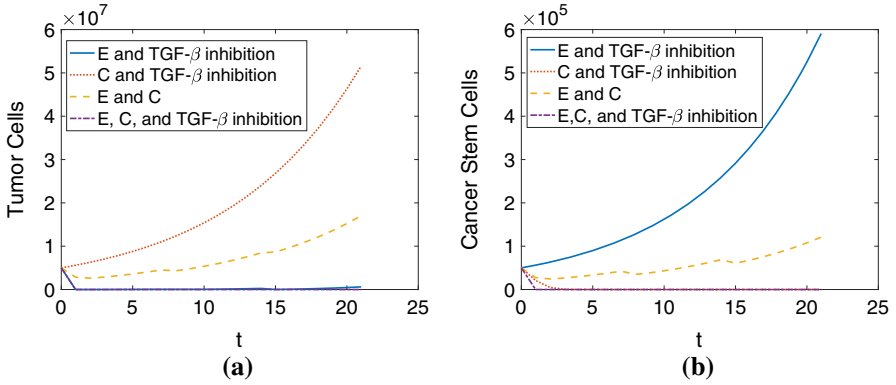

Fig. 12 Comparing outcomes for the number of **(a)** Tumor and **(b)** Stem Cells when i) there are effector cells attacking the tumor and those effector cells are not inhibited by TGF-β (blue), ii) there are effector cells attacking the stem cells and effector cells are not inhibited by TGF-β (red), iii) there are effectors cells attacking both the tumor and stem cells, but those cells are inhibited by TGF-β, and iv) there are effectors cells attacking both the tumor and stem cells, but those cells are inhibited by TGF-β (color figure online)

stem cells is $C = 2 \times 10^5$. In treatment targeting TGF-β, the TGF-β effectiveness is drastically reduced but not fully eliminated (Tang et al. 2020; Hou et al. 2018). In order to incorporate this impact, we assume that the TGF-β is one-thousandth of its normal effectiveness and take $c_1 = .1$ and $c_3 = 10^{-4}$. Otherwise, we use the parameter values listed for Zhang2019 in Table 1. Figure 12 shows the different combinations of treatment. The only time that both the tumor cells and cancer stem cells are eliminated is when both types of effector cells are used and TGF-β has reduced effectiveness. While in this case the system approaches a steady state, it is worth noting that this equilibrium is unstable, which means that if any tumor or stem cells are introduced, there will be a recurrence of the cancer.

6 Conclusions

In this work we present a mathematical model for cancer development that incorporates the impacts of cancer stem cells, in addition to immune cells and tumor cells. The stem cell hypothesis suggests that one of the main reasons for cancer relapse is the presence of cancer stem cells, which initiate tumors post-chemotherapy. Therefore, the cancer stem cell population is essential in order to fully understand the dynamics in the tumor microenvironment and thus also therapies that target the cancer stem cells. Our model allows for several possible treatments: targeting the tumor, targeting the cancer stem cells, inhibiting TGF-β or a combination.

The model proves to be very robust and flexible as it lends itself to be applied to 3 different kinds of cancers with minimal parameter fitting. Moreover a variety of treatments can be incorporated for these cancers without unnecessary complexity.

Sensitivity analysis confirms what we observe in the treatments here, for example CAR-T cell therapies increase the number of effector cells which could also be achieved by increasing the proliferation rate b. The proliferation rate b is negatively correlated with the tumor size. The TGF-β inhibitor therapy causes the effector cells to be blind to the effects of TGF-β causing these cells to be more effective. A similar method would be to reduce the generation rate of TGF-β, a, which we see in the sensitivity analysis is supportive of the tumor growth and thus a reduction would cause the tumor to experience a slower growth. We also show here that cancer stem cell-targeting therapies are very impactful, as there is a high positive correlation between maximal tumor population and v_0, the cancer stem cell division rate. Hence, the sensitivity analysis for the model is informative for developing new therapies.

In the murine studies we use to corroborate the model, neither the cancer stem cells nor the tumor is eliminated under the treatments. We were able to replicate these biological results with our mathematical model. Furthermore, we extended these studies and show through modeling that the combination treatment of the two types of CAR-T cell therapy targeting the cancer stem cells and tumor cells and a TGF-β inhibiting therapy results in full remission. The plethora of biomarker discoveries in the last decade has yielded many likely candidates for further targeted treatment development. As new therapies become available, their respective contributions within the treatment regimen require careful consideration.

Even as a model of increased complexity compared to previous publications, certain key aspects of the tumor immune response were simplified and/or left out of the current model. Future work could address the contributions of both CD4 lymphocytes and CD4 regulatory T cells within the immune response, along with natural killer cells, macrophages and dendritic cells, and their impact on the TME as described in Zheng et al. (2020).

We hope that this model may be used to direct future biological studies into targeted combination therapies, as they generally have fewer serious side effects and are better tolerated among patients.

Data Availability Data are available upon request.

7 Appendix: Stability Analysis

The system of Eq. (1) has four real-valued and biologically sensible equilibrium points, given in Sect. 4. These equilibrium points have been computed using the parameter values by Tang 2020, in Table 1. The Jacobian matrices for each equilibrium point, their eigenvalues and corresponding eigenvectors are given below.

1. **Equilibrium point** $(S^*, T^*, E^*, C^*, B^*, R^*) = (10^7, 9.9 \times 10^8, 0, 0, 845.3, 0)$. As stated in Sect. 4, the system has a line of equilibria on $S^* + T^* = K$; meanwhile, we have observed in numerical simulations, a particular equilibrium on this line. Here, we present the eigenvalues and eigenvectors of this system at this particular point.

   The Jacobian matrix at this equilibrium is:

$$\mathfrak{J}_1 = \begin{bmatrix} -4.9 \times 10^{-4} & -4.9 \times 10^{-4} & 0 & -10 & 0 & 0 \\ -4.8 \times 10^{-2} & -4.8 \times 10^{-2} & -2.3 \times 10^{-1} & 0 & 0 & 0 \\ 0 & 0 & 4.7 \times 10^{-1} & 0 & 0 & 0 \\ 0 & 0 & 0 & 4.8 \times 10^{-1} & 0 & 0 \\ 0 & 2.0 \times 10^{-18} & 0 & 0 & -7.0 \times 10^{-4} & 10^{-8} \\ 0 & 0 & 1.3 \times 10^{-1} & 0 & 0 & -10^{-5} \end{bmatrix}$$

   The eigenvalues are: $(0, -4.9\times10^{-2}, -7.0\times10^{-4}, 4.8\times10^{-1}, -1.0\times10^{-5}, 4.7\times 10^{-1})$ and the corresponding eigenvectors are:

$$\mathbf{v}_1 = \begin{bmatrix} 7.1 \times 10^{-1} \\ -7.1 \times 10^{-1} \\ 0 \\ 0 \\ 0 \\ 0 \end{bmatrix}, \mathbf{v}_2 = \begin{bmatrix} 1.0 \times 10^{-2} \\ 1.0 \\ 0 \\ 0 \\ 0 \\ 0 \end{bmatrix}, \mathbf{v}_3 = \begin{bmatrix} 0.0 \\ 0.0 \\ 0.0 \\ 0.0 \\ -1.0 \\ 0.0 \end{bmatrix}$$

$$\mathbf{v}_4 = \begin{bmatrix} -1.0 \\ 9.0 \times 10^{-2} \\ 0 \\ 4.8 \times 10^{-2} \\ 0 \\ 0 \end{bmatrix}, \mathbf{v}_5 = \begin{bmatrix} 0 \\ 0 \\ 0 \\ 0 \\ 1.4 \times 10^{-5} \\ 1.0 \end{bmatrix}, \mathbf{v}_6 = \begin{bmatrix} 4.3 \times 10^{-4} \\ -4.1 \times 10^{-1} \\ 9.1 \times 10^{-1} \\ 0 \\ 5.1 \times 10^{-10} \\ 2.4 \times 10^{-2} \end{bmatrix}$$

2. **Equilibrium point** $(S^*, T^*, E^*, C^*, B^*, R^*) = (0, 0, 0, 0, 0, 0)$

   The trivial solution,

$$(S^*, T^*, E^*, C^*, B^*, R^*) = (0, 0, 0, 0, 0, 0)$$

   is an unstable equilibrium. The four positive eigenvalues indicate population growth in the directions of the CAR T-cells, the immune cells, tumor and stem cells, all of which are to be expected since the introduction of a few of these cells

would instigate growth for that population. The direction of attraction, for the two negative eigenvalues, is the $B-$axis and a line on the $B-R$ plane, meaning the TGF-β and Tregs tend to stabilize without the presence of effector cells or the tumor. The Jacobian matrix at this equilibrium is:

$$\mathfrak{J}_2 = \begin{bmatrix} 4.9\times10^{-2} & 0 & 0 & 0 & 0 & 0 \\ 0 & 4.7\times10^{-1} & 0 & 0 & 0 & 0 \\ 0 & 0 & -7.0\times10^{-4} & 1.0\times10^{-8} & 0 & 0 \\ 0 & 1.3\times10^{-2} & 0 & -1.0\times10^{-5} & 0 & 0 \\ 3.1\times10^{-1} & 0 & 0 & 0 & 4.5\times10^{-2} & 0 \\ 0 & 0 & 0 & 0 & 0 & 4.8\times10^{-1} \end{bmatrix}$$

The eigenvalues are: $(4.8\times10^{-1}, 4.7\times10^{-1}, 4.9\times10^{-2}, 4.54\times10^{-2}, -7.0\times10^{-4}, -1\times10^{-5})$ and the corresponding eigenvectors are:

$$\mathbf{v}_1 = \begin{bmatrix} 0 \\ 0 \\ 0 \\ 0 \\ 0 \\ 1 \end{bmatrix}, \mathbf{v}_2 = \begin{bmatrix} 0 \\ -1.0 \\ -5.6\times10^{-10} \\ -2.6\times10^{-2} \\ 2.0\times10^{-10} \\ 0 \end{bmatrix}, \mathbf{v}_3 = \begin{bmatrix} -1.2\times10^{-2} \\ 0 \\ 0 \\ 0 \\ -1.0 \\ 0 \end{bmatrix},$$

$$\mathbf{v}_4 = \begin{bmatrix} 0 \\ 0 \\ 0 \\ 0 \\ -1.0 \\ 0 \end{bmatrix}, \mathbf{v}_5 = \begin{bmatrix} 0 \\ 0 \\ 1 \\ 0 \\ 0 \\ 0 \end{bmatrix}, \mathbf{v}_6 = \begin{bmatrix} 0 \\ 0 \\ 1.4\times10^{-5} \\ 1 \\ 0 \\ 0 \end{bmatrix}$$

3. **Equilibrium point** $(S^*, T^*, E^*, C^*, B^*, R^*) = (0, 0, 37.7, 0, 6.7\times10^{-1}, 47179)$ This is a tumor and stem cell-free equilibrium. The three positive eigenvalues have eigenvectors that determine the direction of population growth for all cells, which is expected. The two complex eigenvalues with negative real parts provide a spiral sink-type behavior for the immune cells and TGF-β; without the tumor or the cancer stem cells, the immune system will be in a nonzero equilibrium. The direction for the only attractor is the $B-$axis; without the tumor or Tregs, the TGF-β will stabilize at a low level. The Jacobian matrix at this equilibrium is:

$$\mathfrak{J}_2 = \begin{bmatrix} 4.9\times10^{-2} & 0 & 0 & 0 & 0 & 0 \\ 0 & 0 & 0 & -3.8\times10^{-4} & 4.2\times10^{-2} & 0 \\ 0 & 0 & -7\times10^{-4} & 10^{-8} & 0 & 0 \\ 0 & 1.3\times10^{-2} & 0 & -10^{-6} & 0 & 0 \\ 3.1\times10^{-1} & 0 & 0 & 0 & 4.5\times10^{-2} & 0 \\ 0 & 0 & 0 & 0 & 0 & 1.2\times10^{-2} \end{bmatrix}$$

The eigenvalues are $(4.9 \times 10^{-2}, 4.5 \times 10^{-2}, 1.2 \times 10^{-2}, -5.0 \times 10^{-6} + (2.2 \times 10^{-3})i,$

$-5.0 \times 10^{-6} - (2.2 \times 10^{-3})i, -7.0 \times 10^{-4})$. The corresponding eigenvectors are:

$$\mathbf{v}_1 = \begin{bmatrix} -8.7 \times 10^{-3} \\ -6.4 \times 10^{-1} \\ -3.3 \times 10^{-8} \\ -1.62 \times 10^{-1} \\ -7.5 \times 10^{-1} \\ 0 \end{bmatrix}, \mathbf{v}_2 = \begin{bmatrix} -2.0 \times 10^{-9} \\ -6.6 \times 10^{-1} \\ -4.0 \times 10^{-8} \\ -1.8 \times 10^{-1} \\ -7.3 \times 10^{-1} \\ 0 \end{bmatrix}, \mathbf{v}_3 = \begin{bmatrix} 0 \\ 0 \\ 0 \\ 0 \\ 0 \\ 1 \end{bmatrix},$$

$$\mathbf{v}_4 = \begin{bmatrix} 1.8 \times 10^{-10} + 8.8 \times 10^{-11}\, i \\ 3.9 \times 10^{-4} + 1.7 \times 10^{-1}\, i \\ 1.3 \times 10^{-6} - 4.1 \times 10^{-6}\, i \\ 9.9 \times 10^{-1} \\ 4.8 \times 10^{-11} - 4.4 \times 10^{-10}\, i \\ 0 \end{bmatrix}, \mathbf{v}_5 = \mathbf{v}_4, \mathbf{v}_6 = \begin{bmatrix} -1 \times 10^{-13} \\ -2.0 \times 10^{-10} \\ -1 \\ 7.0 \times 10^{-13} \\ -9.0 \times 10^{-14} \\ 0 \end{bmatrix}$$

4. **Equilibrium point** $(S^*, T^*, E^*, C^*, B^*, R^*) = (0, 10^9, 37.7, 0, 846, 47180)$ The fourth equilibrium is a maximal tumor case where the tumor is at its carrying capacity, which is a saddle. There are two directions of attraction; one of them is the $T-$axis, meaning the tumor population is converging to its carrying capacity, and the other points to a positive tumor, effector cells and TGF-β and an opposite behavior for Tregs. The two complex eigenvalues have negative real parts with corresponding eigenvectors that are a complex scalar multiple of $\mathbf{e}_5$ parallel to the $T-$axis. This freedom is due to the equilibrium not being completely defined and rather the equilibrium of T^* and S^* just must satisfy $T^* + S^* = K$. The Jacobian matrix at this equilibrium is:

$$\mathfrak{J}_4 = \begin{bmatrix} 9.6 \times 10^{-9} & 0 & 0 & 0 & 0 & 0 \\ 0 & 0 & -4.7 \times 10^{-7} & -3.8 \times 10^{-4} & 2.0 \times 10^{-22} & 0 \\ 0 & 0 & -7 \times 10^{-4} & 10^{-}8 & 3.0 \times 10^{-18} & 0 \\ 0 & 1.3 \times 10^{-2} & 0 & -10^{-5} & 0 & 0 \\ -4.5 \times 10^{-2} & -2.4 \times 10^{-1} & 1.1 \times 10^{-2} & 0 & -4.5 \times 10^{-2} & 0 \\ 0 & 0 & 0 & 0 & 0 & 1.2 \times 10^{-2} \end{bmatrix}$$

The eigenvalues are $(-4.5 \times 10^{-2}, 1.2 \times 10^{-2}, -5.0 \times 10^{-6} + (2.1 \times 10^{-3})\, i, -5.0 \times 10^{-6} - (2.1 \times 10^{-3})\, i, -7.0 \times 10^{-4}, 9.6 \times 10^{-9})$. The corresponding eigenvectors are:

$$\mathbf{v}_1 = \begin{bmatrix} 0 \\ 0 \\ 0 \\ 0 \\ 1 \\ 0 \end{bmatrix}, \mathbf{v}_2 = \begin{bmatrix} 0 \\ 0 \\ 0 \\ 0 \\ 0 \\ 1 \end{bmatrix}, \mathbf{v}_3 = \begin{bmatrix} 0 \\ 2.9 \times 10^{-4} - 1.3 \times 10^{-1}\, i \\ 9.8 \times 10^{-7} + 3.1 \times 10^{-6}\, i \\ 7.4 \times 10^{-1} \\ -3.3 \times 10^{-2} + 6.6 \times 10^{-1}\, i \\ 0 \end{bmatrix},$$

$$\mathbf{v}_4 = \mathbf{v}_3, \mathbf{v}_5 = \begin{bmatrix} 0 \\ -6.1 \times 10^{-5} \\ -9.7 \times 10^{-1} \\ 1.1 \times 10^{-3} \\ -2.3 \times 10^{-1} \\ 0 \end{bmatrix}, \mathbf{v}_6 = \begin{bmatrix} -7.1 \times 10^{-1} \\ 0 \\ 0 \\ 0 \\ 7. \times 10^{-1} \\ 0 \end{bmatrix}$$

References

Arciero TL, Kirschner DE (2004) A mathematical model of tumor-immune evasion and sirna treatment. Dis Contin Dyn Syst 4:39–58. https://doi.org/10.3934/dcdsb.2004.4.39

Bashraheel SS, Domling A, Goda SK (2020) Update on targeted cancer therapies, single or in combination, and their fine tuning for precision medicine. Biomedicine & Pharmacotherapy 125:110009. https://doi.org/10.1016/j.biopha.2020.110009

Beretta E, Capasso V, Morozova N (2012) Mathematical modelling of cancer stem cells population behavior. Math Modell Nat Phenom 7(1):279–305. https://doi.org/10.1051/mmnp/20127113

Clara J, Monge C, Yang Y, Takebe N (2020) Targeting signalling pathways and the immune microenvironment of cancer stem cells - a clinical update. Nat Rev Clin Oncol 17(4):204. https://doi.org/10.1038/s41571-019-0293-2

Elliott SL, Kose E, Lewis AL, Steinfeld AE, Zollinger EA (2019) Modeling the stem cell hypothesis: investigating the effects of cancer stem cells and TGF-β on tumor growth. Math Biosci Eng: MBE 16(6):7177–7194. https://doi.org/10.3934/mbe.2019360

Eyvazi S, Farajnia S, Dastmalchi S, Kanipour F, Zarredar H, Bandehpour M (2018) Antibody based EpCAM targeted therapy of cancer, review and update. Curr Cancer Drug Targets 18(9):857–868. https://doi.org/10.2174/1568009618666180102102311

Fasano A, Mancini A, Primicerio M (2016) Tumours with cancer stem cells: a pde model. Math Biosci 272:76–80

Han Y, Sun B, Cai H, Xuan Y (2021) Simultaneously target of normal and stem cells-like gastric cancer cells via cisplatin and anti-CD133 CAR-T combination therapy. Cancer Immunol Immunother. https://doi.org/10.1007/s00262-021-02891-x

Hillen T, Enderling H, Hahnfeldt P (2013) The tumor growth paradox and immune system-mediated selection for cancer stem cells. Bull Math Biol 75(1):161–184

Hou AJ, Chang ZL, Lorenzini MH, Zah E, Chen YY (2018) TGF-β-responsive CAR-T cells promote anti-tumor immune function. Bioeng Trans Med 3(2):75–86. https://doi.org/10.1002/btm2.10097

Johnston MD, Maini PK, Chapman SJ, Edwards CM, Bodmer WF (2010) On the proportion of cancer stem cells in a tumour. J Theor Biol 266(4):708–711

Köse E, Moore S, Ofodile C, Radunskaya A, Swanson ER, Zollinger E (2017) Immuno-kinetics of immunotherapy: dosing with dcs. Lett Biomath 4(1):39–58

Lee Y, Tan Y, Oon C (2018) Molecular targeted therapy: treating cancer with specificity. Eur J Pharmacol 834:188–196. https://doi.org/10.1016/j.ejphar.2018.07.034

Liou G (2019) Cd133 as a regulator of cancer metastasis through the cancer stem cells. Int J Biochem Cell Biol 106:1–7. https://doi.org/10.1016/j.biocel.2018.10.013

Liu X, Johnson S, Liu S, Kanojia D, Yue W, Singh UP, Wang Q, Wang Q, Nie Q, Chen H (2013) Nonlinear growth kinetics of breast cancer stem cells: implications for cancer stem cell targeted therapy. Sci Rep 3(1):2473. https://doi.org/10.1038/srep02473

Louzoun Y, Xue C, Lesinski GB, Friedman A (2014) A mathematical model for pancreatic cancer growth and treatments. J Theor Biol 351:74–82. https://doi.org/10.1016/j.jtbi.2014.02.028
Marino S, Hogue IB, Ray CJ, Kirschner DE (2008) A methodology for performing global uncertainty and sensitivity analysis in systems biology. J Theor Biol 254(1):178–196. https://doi.org/10.1016/j.jtbi.2008.04.011
Marotta LLC, Polyak K (2009) Cancer stem cells: a model in the making. Curr Op Gen Dev 19:44–50. https://doi.org/10.1016/j.gde.2008.12.003
Moo-Young T, Larson J, BA B, Tan M, Hawkins W, Eberlein T, Goedegebuure P, Linehan D (2009) Tumor-derived tgf-β mediates conversion of cd4+foxp3+ regulatory t cells in a murine model of pancreas cancer. J Immunoth 32(1):12–21. https://doi.org/10.1097/CJI.0b013e318189f13c
Morganti S, Tarantino P, Ferraro E, D'Amico P, Duso B, Curigliano G (2019) Next generation sequencing (NGSd): a revolutionary technology in pharmacogenomics and personalized medicine in cancer. Adv Exp Med Biol 1168:9–30. https://doi.org/10.1007/978-3-030-24100-1_2
Mortezaee K (2020) Immune escape: a critical hallmark in solid tumors. Life Sci 258:118110
National Cancer Institute (2020) Cancer statistics. https://www.cancer.gov/about-cancer/understanding/statistics
Piotrowska MJ, Enderling H, van der Heiden U, Mackey MC (2008) Mathematical modeling of stem cells related to cancer. Complex Syst Biomed In: Cancer and Stem Cells, Edited by Thomas Dittmar and Kurt S. Zänker, Nova Science Publishers, Inc., ISBN 978-1-60456-478-5.
Polanczyk M, Walker E, Haley D, Guerrouahen B, Akporiaye E (2019) Blockade of TGF-β signaling to enhance the antitumor response is accompanied by dysregulation of the functional activity of CD4+CD25+Foxp3+ and CD4+CD25-Foxp3+ T cells. J Trans Med 16(1):1–16. https://doi.org/10.1186/s12967-019-1967-3
Radunskaya A, Kim R, Woods T II (2018) Mathematical modeling of tumor immune interactions: a closer look at the role of a PD-L1 inhibitor in cancer immunotherapy. Spora J Biomath 4(1):25–41
Renardy M, Jilkine A, Shahriyari L, Chou CS (2018) Control of cell fraction and population recovery during tissue regeneration in stem cell lineages. J Theor Biol 445:33–50. https://doi.org/10.1016/j.jtbi.2018.02.017
Rodriguez-Brenes IA, Kurtova AV, Lin C, Lee YC, Xiao J, Mims M, Chan KS, Wodarz D (2017) Cellular hierarchy as a determinant of tumor sensitivity to chemotherapy. Cancer Res 77(9):2231. https://doi.org/10.1158/0008-5472.CAN-16-2434
Sahoo P, Yang X, Abler D, Maestrini D, Adhikarla V, Frankhouser D, Cho H, Machuca V, Wang D, Barish M, Gutova M, Branciamore S, Brown CE, Rockne RC (2020) Mathematical deconvolution of CAR T-cell proliferation and exhaustion from real-time killing assay data. J R Soc Interface 17(162):20190734
Scarfò I, Maus M (2017) Current approaches to increase CAR T cell potency in solid tumors: targeting the tumor microenvironment. J Immunoth Cancer 5:28. https://doi.org/10.1186/s40425-017-0230-9
Sigal D, Przedborski M, Sivaloganathan D, Kohandel M (2019) Mathematical modelling of cancer stem cell-targeted immunotherapy. Math Biosci 318:108269. https://doi.org/10.1016/j.mbs.2019.108269
Soetaert K, Petzoldt T (2010) Inverse modelling, sensitivity and monte carlo analysis in R using package FME. J Stat Softw 33(3):1–28
Tang N, Cheng C, Zhang X, Qiao M, Li N, Mu W, Wei XF, Han W, Wang H (2020) TGF-β inhibition via CRISPR promotes the long-term efficacy of CAR T cells against solid tumors. JCI Insight. https://doi.org/10.1172/jci.insight.133977
Tomasetti C, Vogelstein B (2015) Variation in cancer risk among tissues can be explained by the number of stem cell divisions. Science 347(6217):78–81. https://doi.org/10.1126/science.1260825
Wang J, Lei K, Han F (2018) Tumor microenvironment: recent advances in various cancer treatments. Eur Rev Med Pharmacol Sci 22(12):3855–3864
Weekes SL, Barker B, Bober S, Cisneros K, Cline J, Thompson A, Hlatky L, Hahnfeldt P, Enderling H (2014) A multicompartment mathematical model of cancer stem cell-driven tumor growth dynamics. Bull Math Biol 76(7):1762–1782
Weiss LD, Komarova NL, Rodriguez-Brenes IA (2017) Mathematical modeling of normal and cancer stem cells. Curr Stem Cell Rep 3(3):232–239
Wilson S, Levy D (2012) A mathematical model of the enhancement of tumor vaccine efficacy by immunotherapy. Bull Math Biol 74(7):1485–1500. https://doi.org/10.1007/s11538-012-9722-4
Wodarz D (2018) Effect of cellular de-differentiation on the dynamics and evolution of tissue and tumor cells in mathematical models with feedback regulation. J Theor Biol 448:86–93. https://doi.org/10.1016/j.jtbi.2018.03.036

Youssefpour H, Li X, Lander AD, Lowengrub JS (2012) Multispecies model of cell lineages and feedback control in solid tumors. J Theor Biol 304:39–59. https://doi.org/10.1016/j.jtbi.2012.02.030

Zhang BL, Li D, Gong YL, Huang Y, Qin DY, Jiang L, Liang X, Yang X, Gou HF, Wang YS, Wei YQ, Wang W (2019) Preclinical evaluation of chimeric antigen receptor-modified t cells specific to epithelial cell adhesion molecule for treating colorectal cancer. Hum Gene Ther 30(4):402–412. https://doi.org/10.1089/hum.2018.229

Zheng Y, Chen Z, Han Y, Han L, Zou X, Zhou B, Hu R, Hao J, Bai S, Xiao H, Li W, Bueker A, Ma Y, Xie G, Yang J, Chen S, Li H, Cao J, Shen L (2020) Immune suppressive landscape in the human esophageal squamous cell carcinoma microenvironment. Nat Commun 11(1):1–17

Publisher's Note Springer Nature remains neutral with regard to jurisdictional claims in published maps and institutional affiliations.